arXiv:1402.0656v1 [nucl-th] 4 Feb 2014

Pion photo- and electroproduction in relativistic baryon ChPT

Lothar Tiator[1,a], Stefan Scherer[1], and Marius Hilt[1]

[1] *Institut für Kernphysik, Johannes Gutenberg-Universität Mainz, D-55099 Mainz*

Abstract. We present a calculation of pion photo- and electroproduction in manifestly Lorentz-invariant baryon chiral perturbation theory up to and including order q^4. We fix the low-energy constants by fitting experimental data in all available reaction channels. Our results can be accessed via a web interface, the so-called chiral MAID.

1 Introduction

In the middle of the 1980s, renewed interest in neutral pion photoproduction at threshold was triggered by experimental data from Saclay and Mainz, which indicated a serious disagreement with the predictions for the *s*-wave electric dipole amplitude E_{0+} based on current algebra and PCAC. This discrepancy was explained with the aid of ChPT . Pion loops, which are beyond the current-algebra framework, generate infrared singularities in the scattering amplitude which then modify the predicted low-energy expansion of E_{0+}. Subsequently, several experiments investigated pion photo- and electroproduction in the threshold region were performed at Mainz, MIT-Bates, Saskatoon and TRIUMF, and on the theoretical side, all of the different reaction channels of pion photo- and electroproduction near threshold were extensively investigated by Bernard, Kaiser and Meißner within the framework of heavy-baryon chiral perturbation theory (HBChPT). For a complete list of references, see Ref. [1].

In the beginning, the manifestly Lorentz-invariant or relativistic formulation of ChPT (RChPT) was abandoned, as it seemingly had a problem with respect to power counting when loops containing internal nucleon lines come into play. Therefore, HBChPT became a standard tool for the analysis of pion photo- and electroproduction in the threshold region. In the meantime, the development of the infrared regularization (IR) scheme [2] and the extended on-mass-shell (EOMS) scheme [3] offered a solution to the power-counting problem, and RChPT became popular again.

We present a calculation of pion photo- and electroproduction on the nucleon in manifestly Lorentz-invariant baryon chiral perturbation theory up to and including chiral order p^4. Within this framework we analyze π^0 and charged photo- and electroproduction data in the threshold region, most of them obtained at the Mainz Microtron, MAMI. We also compare our results with the dynamical model DMT [4] and the unitary and causal effective field theory of Gasparyan and Lutz [5].

2 Pion photo- and electroproduction

For pion photoproduction with polarized photons from an unpolarized target without recoil polarization detection, the cross section can be written in the following way with the unpolarized cross section

[a] e-mail: tiator@kph.uni-mainz.de

σ_0 und the photon beam asymmetry Σ.

$$\frac{d\sigma}{d\Omega} = \sigma_0 \left(1 - P_T \Sigma \cos 2\varphi\right). \tag{1}$$

For π^0 photoproduction on the proton, both observables are very precisely measured in the threshold region, allowing an almost model independent partial wave analysis [6].

For pion electroproduction, in the one-photon-exchange approximation, the differential cross section can be written as

$$\frac{d\sigma}{d\mathcal{E}_f d\Omega_f d\Omega_\pi^{\rm cm}} = \Gamma \frac{d\sigma_v}{d\Omega_\pi^{\rm cm}}, \tag{2}$$

where Γ is the virtual photon flux and $d\sigma_v/d\Omega_\pi^{\rm cm}$ is the pion production cross section for virtual photons.

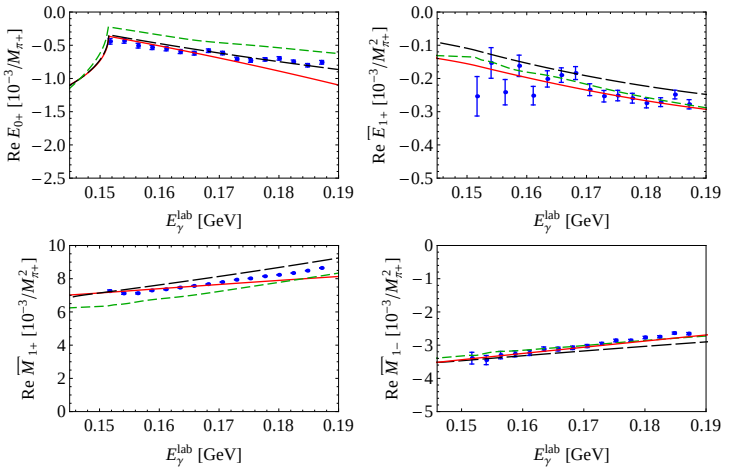


Figure 1. (Color online) S- and reduced P-wave multipoles for $\gamma + p \to p + \pi^0$. The solid (red) curves show our RChPT calculations at $O(q^4)$. The short-dashed (green) and long-dashed (black) curves are the predictions of the DMT model [4] and the GL model [5], respectively. The data are from Ref. [6].

For an unpolarized target and without recoil polarization detection, the virtual-photon differential cross section for pion production can be further decomposed as

$$\frac{d\sigma_v}{d\Omega_\pi} = \frac{d\sigma_T}{d\Omega_\pi} + \epsilon \frac{d\sigma_L}{d\Omega_\pi} + \sqrt{2\epsilon(1+\epsilon)} \frac{d\sigma_{LT}}{d\Omega_\pi} \cos\Phi_\pi + \epsilon \frac{d\sigma_{TT}}{d\Omega_\pi} \cos 2\Phi_\pi + h\sqrt{2\epsilon(1-\epsilon)} \frac{d\sigma_{LT'}}{d\Omega_\pi} \sin\Phi_\pi, \tag{3}$$

where it is understood that the variables of the individual virtual-photon cross sections $d\sigma_T/d\Omega_\pi$ etc. refer to the cm frame. For further details, especially concerning polarization observables, see [7].

3 Results and Conclusions

First, we show the real parts of the S and P waves in Fig. 1 together with single-energy fits of Ref. [6]. For comparison, we also show the predictions of the Dubna-Mainz-Taipei (DMT) model [4] and the covariant, unitary, chiral approach of Gasparyan and Lutz (GL) [5]. The multipole E_{0+} agrees nicely

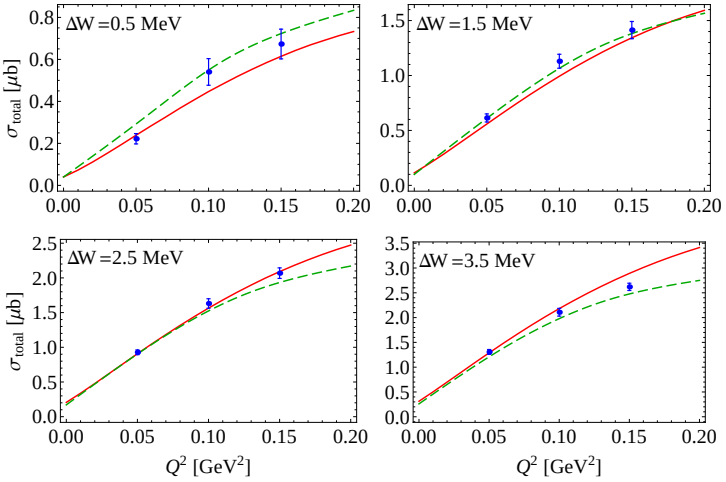


Figure 2. (Color online) Total cross sections in μb as a function of Q^2 for different cm energies above threshold ΔW in MeV. The data are from Refs. [8].

with the data in the fitted energy range. The reduced P waves $\overline{E}_{1+} = E_{1+}/q_\pi$ and $\overline{M}_{1-} = M_{1-}/q_\pi$ with the pion momentum q_π in the c.m. frame agree for even higher energies with the single energy fits. The largest deviation can be seen in $\overline{M}_{1+}$. This multipole is related to the Δ resonance and the rising of the data above 170 MeV can be traced back to the influence of this resonance. As we did not include the Δ explicitly, this calculation is not able to fully describe its impact on the multipole.

For electroproduction, in Fig. 2 we show the total cross section $\sigma_{total} = \sigma_T + \epsilon\sigma_L$ in the threshold region together with the experimental data [8], and in Fig. 3 we compare our results for the coincidence cross sections σ_0, σ_{TT}, σ_{LT} and the beam asymmetry $A_{LT'}$ with the experimental data of Ref. [9] and the results of HBChPT [11] and the DMT model [4]. In general, the DMT model gives a very good description of all observables and amplitudes in the threshold region and can be used as a guideline for theoretical calculations in cases where experimental data do not exist. The HBChPT calculations shown in Fig. 3 were fitted to these data and are taken from Ref. [9]. In contrast, our RChPT calculation is not fitted to these data, as all LECs were already determined with other data before. While HBChPT gives a better description for the unpolarized cross section $\sigma_0(\Theta_\pi) = \sigma_T(\Theta_\pi) + \epsilon\sigma_L(\Theta_\pi)$ than our RChPT calculation, a comparison with the separated cross sections σ_T and σ_L shows that this is mainly due to a longitudinal cross section which is much too small in the HBChPT fit. For the other observables σ_{LT}, σ_{TT}, and the asymmetry $A_{LT'}$, RChPT compares much better to the data than HBChPT. It is interesting to note that the asymmetry $A_{LT'}$ depends only weakly on LECs and has an important contribution from the parameter-free pion loop contribution.

For $\Theta_\pi = \Phi_\pi = 90^\circ$ and for $\epsilon \approx 1$ we find in very good approximation the simple form

$$A_{LT'}(90^\circ) \approx \frac{\sqrt{2\epsilon(1-\epsilon)}\,\sqrt{Q^2/k_0^2}\,(-P_2)\,\mathrm{Im}(L_{0+})}{P_3^2}\,, \tag{4}$$

where $P_2 = 3E_{1+} - M_{1+} + M_{1-}$ and $P_3 = 2M_{1+} + M_{1-}$. Therefore, this asymmetry is very sensitive to the imaginary part of the longitudinal S wave L_{0+}, hence practically independent of LECs. This is

very similar to the case of the target asymmetry T for $\gamma p \to p\pi^0$ which we discussed in Ref. [10]. There, the target asymmetry is shown to be the ideal polarization observable to measure $\mathrm{Im}(E_{0+})$.

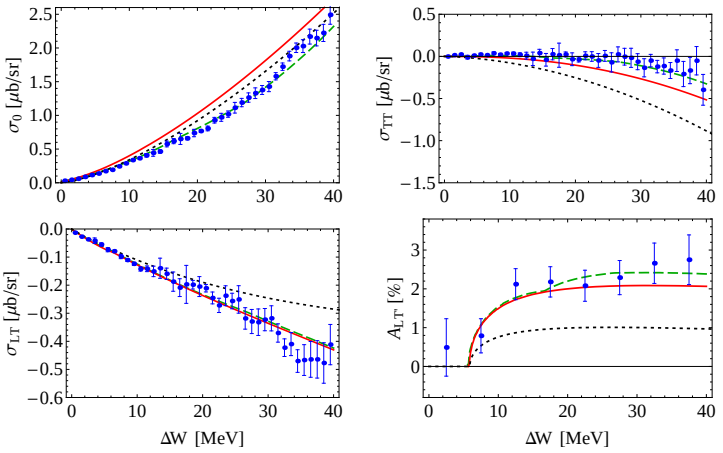


Figure 3. (Color online) Coincidence cross sections σ_0, σ_{TT}, and σ_{LT} in μb/sr and beam asymmetry $A_{LT'}$ in % at constant $Q^2 = 0.05$ GeV^2, $\Theta_\pi = 90°$, $\Phi_\pi = 90°$, and $\epsilon = 0.93$ as a function of ΔW above threshold. The solid (red) lines show our RChPT calculations at $O(q^4)$ and the dotted (black) lines are the heavy-baryon ChPT calculations of Ref. [11]. The dashed (green) curves are obtained from the DMT model [4]. The data are from Ref. [9].

In summary we have shown for the first time a chiral perturbation theory approach that consistently can describe all pion photo- and electroproduction processes in the threshold region equally well. Our relativistic chiral perturbation theory calculation is also online available within the MAID project as ChiralMaid under http://www.kph.uni-mainz.de/MAID/.

Acknowledgements

This work was supported by the Deutsche Forschungsgemeinschaft (SFB 443 and 1044).

References

[1] M. Hilt, B. C. Lehnhart, S. Scherer and L. Tiator, Phys. Rev. C **88**, 055207 (2013).
[2] T. Becher and H. Leutwyler, Eur. Phys. J. C **9**, 643 (1999).
[3] J. Gegelia and G. Japaridze, Phys. Rev. D **60**, 114038 (1999).
[4] S. S. Kamalov, G.-Y. Chen, S.-N. Yang, D. Drechsel, and L. Tiator, Phys. Lett. B **522**, 27 (2001).
[5] A. Gasparyan and M. F. M. Lutz, Nucl. Phys. A **848**, 126 (2010).
[6] D. Hornidge *et al.* [A2 and CB-TAPS Collaboration], Phys. Rev. Lett. **111**, 062004 (2013).
[7] D. Drechsel and L. Tiator, J. Phys. G **18**, 449 (1992).
[8] H. Merkel, PoS CD **09**, 112 (2009) and H. Merkel *et al.*, arXiv:1109.5075 [nucl-ex].
[9] M. Weis *et al.* [A1 Collaboration], Eur. Phys. J. A **38**, 27 (2008).
[10] M. Hilt, S. Scherer and L. Tiator, Phys. Rev. C **87**, 045204 (2013).
[11] V. Bernard, N. Kaiser, and U.-G. Meißner, Phys. Lett. B **383**, 116 (1996).